CONSTRAINING THE STRUCTURE OF GAMMA-RAY BURST JETS
THROUGH THE $\log N$–$\log S$ DISTRIBUTION

Dafne Guetta,[1,2] Jonathan Granot,[3] and Mitchell C. Begelman[2]

ABSTRACT

A general formalism is developed for calculating the luminosity function and the expected number N of observed gamma-ray bursts (GRBs) above a peak photon flux S for an arbitrary GRB jet structure. This formalism directly provides the true GRB rate for any jet model, instead of first calculating the GRB rate assuming isotropic emission and then introducing a "correction factor" to account for effects of the GRB jet structure, as was done in previous works. We apply it to the uniform jet (UJ) and universal structured jet (USJ) models for the structure of GRB jets and perform fits to the observed $\log N$–$\log S$ distribution from the GUSBAD catalog, which contains 2204 BATSE bursts. We allow for a scatter in the peak luminosity L for a given jet half-opening angle θ_j (viewing angle $\theta_{\rm obs}$) in the UJ (USJ) model, which is implied by observations. A core angle θ_c and an outer edge at $\theta_{\rm max}$ are introduced for the structured jet, and a finite range of opening angles $\theta_{\rm min} \leq \theta_j \leq \theta_{\rm max}$ is assumed for the uniform jets. The efficiency for producing γ-rays, ϵ_γ, and the energy per solid angle in the jet, ϵ, are allowed to vary with θ_j ($\theta_{\rm obs}$) in the UJ (USJ) model, $\epsilon_\gamma \propto \theta^{-b}$ and $\epsilon \propto \theta^{-a}$. We find that a single power-law luminosity function provides a good fit to the data. Such a luminosity function arises naturally in the USJ model, while in the UJ model it implies a power-law probability distribution for θ_j, $P(\theta_j) \propto \theta_j^{-q}$. The value of q cannot be directly determined from the fit to the observed $\log N$–$\log S$ distribution, and an additional assumption on the value of a or b is required. Alternatively, an independent estimate of the true GRB rate would enable one to determine a, b, and q. The implied values of θ_c (or $\theta_{\rm min}$) and $\theta_{\rm max}$ are close to the current observational limits. The true GRB rate for the USJ model is found to be $R_{\rm GRB}(z=0) = 0.86^{+0.14}_{-0.05}$ Gpc^{-3} yr^{-1} (1 σ), while for the UJ model it is higher by a factor $f(q)$, which strongly depends on the unknown value of q.

Subject headings: cosmology: observations — gamma rays: bursts — gamma rays: theory — ISM: jets and outflows

Online material: color figures

1. INTRODUCTION

There are several lines of evidence in favor of jets in gamma-ray bursts (GRBs). For GRBs with known redshift z, the fluence can be used to determine the total energy output in γ-rays assuming spherical symmetry, $E_{\gamma,\rm iso}$. The values of $E_{\gamma,\rm iso}$ that were inferred in this way sometimes approached, and in one case (GRB 991023) even exceeded, $M_\odot c^2$. Such high energies are very hard to reconcile with progenitor models involving stellar mass objects. A nonspherical, collimated outflow (i.e., a jet) can significantly reduce the total energy output in γ-rays compared to $E_{\gamma,\rm iso}$, since in this case the γ-rays are emitted only into a small fraction, $f_b \ll 1$, of the total solid angle. A more direct (and probably the best so far) line of evidence in favor of jets in GRBs is from achromatic breaks in the afterglow light curves (Rhoads 1997, 1999; Sari et al. 1999).

Despite the large progress in GRB research since the discovery of the afterglow emission in early 1997, the structure of GRB jets is still an open question. This is a particularly interesting and important question, since it affects the total energy output and event rate of GRBs, as well as the requirements from the central engine that accelerates and collimates these relativistic jets.

The leading models for the jet structure are (1) the uniform jet (UJ) model (Rhoads 1997, 1999; Panaitescu & Meszáros 1999; Sari et al. 1999; Kumar & Panaitescu 2000; Moderski et al. 2000; Granot et al. 2001, 2002), where the energy per solid angle ϵ and the initial Lorentz factor Γ_0 are uniform within some finite half-opening angle θ_j and sharply drop outside of θ_j; and (2) the universal structured jet (USJ) model (Lipunov et al. 2001; Rossi et al. 2002; Zhang & Mészáros 2002), where ϵ and Γ_0 vary smoothly with the angle θ from the jet symmetry axis. In the UJ model the different values of the jet break time t_j in the afterglow light curve arise mainly because of different θ_j (and to a lesser extent because of different ambient densities). In the USJ model, all GRB jets are intrinsically identical, and the different values of t_j arise mainly because of different viewing angles $\theta_{\rm obs}$ from the jet axis [in fact, the expression for t_j is similar to that for a uniform jet with $\epsilon \rightarrow \epsilon(\theta_{\rm obs})$ and $\theta_j \rightarrow \theta_{\rm obs}$]. The observed correlation $t_j \propto E_{\gamma,\rm iso}^{-1}$ (Frail et al. 2001; Bloom et al. 2003) implies a roughly constant true energy E between different GRB jets in the UJ model, and $\epsilon \propto \theta^{-2}$ outside of some core angle θ_c in the USJ model (Rossi et al. 2002; Zhang & Mészáros 2002).[4] The probability distribution of jet half-opening angles between different GRBs in the UJ model, $P(\theta_j)$, is not given a priori by the model and is a free function to be determined by observations.

Several methods have been used so far in order to constrain the structure of GRB jets and help distinguish between the

[1] Racah Institute for Physics, The Hebrew University, Jerusalem 91904, Israel; dafne@arcetri.astro.it.
[2] JILA, 440 UCB, University of Colorado, Boulder, CO 80309; mitch@jila.colorado.edu.
[3] Institute for Advanced Study, Olden Lane, Princeton, NJ 08540; granot@ias.edu; and KIPAC, Stanford University, P.O. Box 20450, Mail Stop 29, Stanford, CA 94309; granot@slac.stanford.edu.

[4] The latter is obtained assuming that the efficiency in producing γ-rays, ϵ_γ, does not depend on θ. We later examine the consequences of relaxing this assumption.

UJ model and the USJ model. The afterglow light curves are similar for the UJ and USJ models, but nevertheless some differences still exist that might help distinguish between them (Kumar & Granot 2003; Granot & Kumar 2003). Afterglow light curves also constrain the jet structure in the USJ model, as discussed in § 3. This method requires a very good and dense monitoring of the afterglow light curves, especially near the jet break time t_j. Another possible way to distinguish between these two models for the jet structure is through the different expected evolution of the linear polarization during the afterglow (Rossi et al. 2004). However, some difficulties and complications exist in this method, such as the poor quality of most polarization light curves and a possible ordered magnetic field component that might cause polarization that is not related to the jet structure (Granot & Königl 2003). The distribution of viewing angles θ_{obs}, inferred from the observed values of t_j, has been used to argue in favor of the USJ model (Perna et al. 2003). However, when the known redshifts of the same sample of GRBs are also taken into account, there is a very poor agreement with the predictions of the USJ model (Nakar et al. 2004). In order to reach strong conclusions using this method, a large and uniform sample of GRBs with known redshifts is needed, such as the one expected from *Swift*.

In this paper we use the observed $\log N - \log S$ distribution (the number N of GRBs above a limiting peak photon flux S) in order to constrain the jet structure. A somewhat similar analysis was done by Guetta et al. (2005). They found that the observed $\log N - \log S$ distribution rules out the USJ model because of the paucity of GRBs with small peak fluxes compared to the prediction of the USJ model, and fitted a double power-law luminosity function for the UJ model. Firmani et al. (2004) tried to constrain the redshift evolution of the GRB rate and luminosity function, using the $\log N - \log S$ distribution (as well as the redshift distribution derived from the luminosity-variability relation).

This paper improves on previous works by (1) allowing the efficiency in producing γ-rays to be a function of the angle θ, $\epsilon_\gamma = \epsilon_\gamma(\theta)$, and varying $\epsilon(\theta)$ accordingly, using the Frail et al. (2001) relation; (2) including an internal dispersion in the peak isotropic equivalent luminosity L at any given angle θ; (3) introducing an inner core angle θ_c and an outer edge θ_{max} in the USJ model; and (4) using a larger and more uniform GRB sample.

In § 2 we allow ϵ_γ and ϵ to vary with θ and derive the constraints on the power-law indices that are implied by the Frail et al. (2001) relation. The formalism for calculating the luminosity function and the observed GRB rate as a function of the limiting flux for different jet structures is derived in § 3. In §§ 4 and 5 we compare the observed $\log N - \log S$ distribution to the predictions of the USJ and UJ models, respectively. Our results are discussed in § 6.

2. THE ENERGY AND GAMMA-RAY EFFICIENCY DISTRIBUTIONS

The efficiency for producing γ-rays, ϵ_γ, is taken to be a function of the angle θ from the jet symmetry axis in the USJ model, and a function of the jet half-opening angle θ_j in the UJ model. For convenience we assume a power-law dependence on θ in the USJ model, $\epsilon_\gamma(\theta) = \Theta(\theta_{\mathrm{max}} - \theta)\epsilon_{\gamma,0}\min[1, (\theta/\theta_c)^{-b_{\mathrm{USJ}}}]$, where $\Theta(x)$ is the Heaviside step function. An outer edge at θ_{max} has been introduced, as well as a core angle, $\theta_c \gtrsim 1/\Gamma_{\mathrm{max}} \sim 5 \times 10^{-4}$ rad, which is needed in order to avoid a divergence at $\theta = 0$. Here $\Gamma_{\mathrm{max}} \sim 2000$ is the maximum value of the Lorentz factor to which the fireball can be accelerated (Guetta et al.

2001). For the UJ model $P(\theta_j)$ is restricted to a finite range of values, $\theta_{\mathrm{min}} \leq \theta_j \leq \theta_{\mathrm{max}}$, and in analogy to the USJ model we chose $\epsilon_\gamma(\theta_j) = \Theta(\theta_{\mathrm{max}} - \theta_j)\Theta(\theta_j - \theta_{\mathrm{min}})\epsilon_{\gamma,0}(\theta_j/\theta_{\mathrm{min}})^{-b_{\mathrm{UJ}}}$.

The energy per solid angle is also assumed to behave as a power law, $\epsilon(\theta) = \Theta(\theta_{\mathrm{max}} - \theta)\epsilon_0\min[1, (\theta/\theta_c)^{-a_{\mathrm{USJ}}}]$ in the USJ model and $\epsilon(\theta) = \Theta(\theta_{\mathrm{max}} - \theta_j)\Theta(\theta_j - \theta_{\mathrm{min}})\epsilon_0(\theta_j/\theta_{\mathrm{min}})^{-a_{\mathrm{UJ}}}$ in the UJ model. The power-law indices a and b can be different between the USJ and UJ models (as is emphasized by the different subscript for the two models), and we also consider different values for a and b within each model.

The external mass density is taken to be a power law in the distance R from the central source, $\rho_{\mathrm{ext}} = AR^{-k}$. For a constant efficiency ϵ_γ ($b = 0$) the observed correlation $t_j \propto E_{\gamma,\mathrm{iso}}^{-1}$ (Frail et al. 2001; Bloom et al. 2003) implies $a = 2$ (Rossi et al. 2002; Zhang & Mészáros 2002). In the following, we allow b to vary and find the joint constraint that the Frail et al. (2001) relation puts on a and b.

The afterglow emission becomes prominent when the GRB ejecta sweeps enough of the external medium to decelerate significantly. After this time most of the energy is in the shocked external medium, and energy conservation implies

$$\epsilon \approx \Gamma^2 \mu c^2 = \Gamma^2 A c^2 R^{3-k}/(3-k), \qquad (1)$$

where μ is the swept-up rest mass per solid angle.

In the UJ model $\Gamma(t_j) \sim 1/\theta_j$ (Rhoads 1997; Sari et al. 1999), while in the USJ model $\Gamma(t_j) \sim 1/\theta_{\mathrm{obs}}$ (Rossi et al. 2002; Zhang & Mészáros 2002) and the emission around t_j is dominated by material close to our line of sight. Together with the relation $R \sim 4\Gamma^2 ct$, we have

$$t_j \approx \frac{1}{4c}\left[\frac{(3-k)\epsilon(\theta)}{Ac^2}\right]^{1/(3-k)} \theta^{2(4-k)/(3-k)} \propto \theta^{[2(4-k)-a]/(3-k)}, \qquad (2)$$

where $\theta = \theta_j$ for the UJ model and $\theta = \theta_{\mathrm{obs}}$ for the USJ model. Now, in order to satisfy the observed correlation,[5] $t_j \propto E_{\gamma,\mathrm{iso}}^{-1} \propto \theta^{a+b}$, we must have

$$\lambda \equiv a + b = \frac{2(4-k)-a}{3-k}. \qquad (3)$$

Therefore, if we allow the efficiency and the energy per solid angle to vary in this way, we obtain the condition $b = (2 - a)(4 - k)/(3 - k)$ or $a = 2 - b(3 - k)/(4 - k)$ in order to reproduce the observed correlation of Frail et al. (2001).

For the USJ model, interesting constraints on the power-law index a_{USJ} of the energy per solid angle have been derived from the shape of the afterglow light curve (Granot & Kumar 2003; Kumar & Granot 2003). For $a_{\mathrm{USJ}} \lesssim 1.5$ the change in the temporal decay index across the jet break is too small compared to observations, while for $a_{\mathrm{USJ}} \gtrsim 2.5$ there is a very pronounced flattening of the light curve before the jet break, which is not observed. The latter feature arises since the inner parts of the jet near the core, where ϵ is the largest, become visible. This explains why this feature becomes more pronounced for $a_{\mathrm{USJ}} > 2$, where most of the energy in the jet is concentrated at small angles, near the core. There is no sharp borderline where the light curves change abruptly. Instead, the light curves change

---

[5] We have $E_{\gamma,\mathrm{iso}}^{-1} \propto \theta^{a+b}$, since $E_{\gamma,\mathrm{iso}}(\theta) = 4\pi\epsilon(\theta)\epsilon_\gamma(\theta)$. The peak isotropic equivalent luminosity is given by $L = E_{\gamma,\mathrm{iso}}/T$, where T is the effective duration of the GRB, which is assumed to be uncorrelated with L so that L has the same θ dependence as $E_{\gamma,\mathrm{iso}}$.

smoothly with the parameter a_{USJ}. Altogether, the observed shape of the afterglow light curve constrains the parameter a_{USJ} to be in the range $1.5 \lesssim a_{USJ} \lesssim 2.5$. It is important to stress that this constraint applies only to the USJ model and not to the UJ model, since in the former a_{USJ} determines the structure of an individual jet (and therefore affects the light curves), while in the latter the structure of an individual jet is fixed and a_{UJ} only affects how the uniform ϵ changes between different jets of different half-opening angles θ_j.

One might also try to constrain the power-law index b of the γ-ray efficiency ϵ_γ from observations. This would, of course, apply to both the USJ model and the UJ model. The way in which this has been done so far is by taking $\epsilon_\gamma = E_{\gamma,iso}/(E_{\gamma,iso} + E_{k,iso})$, where $E_{k,iso}$ is the initial value of the isotropic equivalent kinetic energy. However, it is hard to evaluate $E_{k,iso}$ very accurately. It is usually evaluated from afterglow observations several hours to days after the GRB and can provide an estimate accurate to within a factor of ~ 2 or so for the kinetic energy at that time. An additional and potentially larger uncertainty arises, since at early times there is fast cooling and radiative losses might reduce the initial kinetic energy by up to an order of magnitude or so. This can be taken into account, but introduces an additional uncertainty in the value of $E_{k,iso}$ that is estimated in this way.

Panaitescu & Kumar (2001, 2002) evaluated $E_{k,iso}$ from a fit to the broadband afterglow data for 10 different GRBs and obtained $\epsilon_\gamma \gtrsim 0.5$ for most of these GRBs and $\epsilon_\gamma \gtrsim 0.1$ for all of them. There seems to be no particular correlation with θ, but because of the small number of bursts and the reasonably large uncertainty in $E_{k,iso}$, there might still be some intrinsic correlation. Lloyd-Ronning & Zhang (2004) used the X-ray luminosity at 10 hr to estimate the kinetic energy at that time and used a simple analytic expression (Sari 1997) to account for the radiative losses. In this way they estimated ϵ_γ for 17 GRBs and one X-ray flash (XRF 020903). Their Figure 6 suggests that ϵ_γ decreases with θ, although they claim that this is not statistically significant. Since most of the estimates for ϵ_γ are $\gtrsim 0.5$ and are for small values of θ, and since $\epsilon_\gamma < 1$ by definition, this suggests $b \gtrsim 0$ (otherwise we would have $\epsilon_\gamma > 1$ at large θ, which is impossible). Moreover, Figure 6 of Lloyd-Ronning & Zhang (2004) suggests that $0 \lesssim b \lesssim 1$. If we assume that $0 \lesssim b \lesssim 1$, then equation (3) would imply $1.25 \lesssim a \lesssim 2$, $2 \lesssim \lambda \lesssim 2.25$ for $k = 0$, and $1.5 \lesssim a \lesssim 2$, $2 \lesssim \lambda \lesssim 2.5$ for $k = 2$.

3. LUMINOSITY FUNCTION FOR DIFFERENT JET STRUCTURES

For simplicity, we assume that the emission from the GRB jet is axially symmetric, so that the observed luminosity depends only on the viewing angle θ from the jet axis and does not depend on the azimuthal angle ϕ. It is convenient to define the probability distribution $P(L|\theta)$, where $P(L|\theta)dL$ is the probability for an isotropic equivalent luminosity between L and $L + dL$, when viewing the jet from an angle θ. Naturally, we must have $\int P(L|\theta)dL = 1$ for any value of θ. The probability of viewing the jet from an angle between θ and $\theta + d\theta$ is simply $P(\theta)d\theta = \sin\theta d\theta$, and $\int_0^{\pi/2} P(\theta)d\theta = 1$. Averaging over the viewing angle θ we obtain the overall probability distribution for L,

$$P(L) = \int_0^{\pi/2} P(\theta)P(L|\theta)\,d\theta = \int_0^1 P(L|\theta)\,d\cos\theta. \quad (4)$$

For a universal GRB jet structure, i.e., if all GRB jets have the same intrinsic properties, then equation (4) represents the GRB luminosity function.

As a simple and very useful example, let us consider a universal structured jet model where[6] $P(L|\theta) = \delta[L - L(\theta)]$ and $L(\theta) = L_0(\theta/\theta_0)^{-\lambda}$. Using equation (4) this implies $P(L) = (\theta_0/\lambda L_0)(L/L_0)^{-1-1/\lambda}\sin\theta(L)$, where $\theta(L) = \theta_0(L/L_0)^{-1/\lambda}$, and for $\theta(L) \ll 1$ it reduces to $P(L) \approx (\theta_0^2/\lambda L_0)(L/L_0)^{-1-2/\lambda}$. Alternatively, one may assume $P(L) = C_0 L^{-\eta}$,[7] where $\eta = 1 + 2/\lambda$ and $C_0 \sim \lambda^{-1}\theta_0^2 L_0^{\eta-1}$ is determined by the normalization condition, $\int P(L)dL = 1$.

An important point to stress here is that $P(L)$ represents the average over all possible viewing angles. Even if the jet is assumed to have a sharp outer edge at some finite angle θ_{max}, with some probability distribution $P^*(L)$ for $\theta < \theta_{max}$, such that $P^*(L) = (1 - \cos\theta_{max})^{-1}\int_0^{\theta_{max}} d\theta \sin\theta P(L|\theta)$ and $P(L|\theta > \theta_j) = \delta(L)$, then $P(L) = (1 - \cos\theta_{max})P^*(L) + \cos\theta_{max}\delta(L)$.

If the GRB jet structure is not universal, and $P(L|\theta)$ depends on additional parameters that describe the jet structure, then equation (4) needs to be averaged over these parameters in order to obtain the GRB luminosity function. For example, for a uniform jet of half-opening angle θ_j, we have $P(L|\theta, \theta_j) = \Theta(\theta_j - \theta)P^*(L|\theta_j) + \Theta(\theta - \theta_j)\delta(L)$, where $P^*(L|\theta_j)$ is the probability distribution of L inside the jet (at $\theta < \theta_j$) for a given value of θ_j. In this case, if $P(\theta_j)$ is the probability distribution for θ_j, then the GRB luminosity function is given by

$$P(L) = \int_0^{\pi/2} P(\theta_j)\,d\theta_j \int_0^{\pi/2} P(\theta)d\theta P(L|\theta, \theta_j)$$

$$= \int_0^{\pi/2} P(\theta_j)\,d\theta_j \left[(1 - \cos\theta_j)P^*(L|\theta_j) + \cos\theta_j\delta(L)\right]. \quad (5)$$

In analogy with the USJ model, we assume for the UJ model that $\epsilon = \epsilon_0(\theta_j/\theta_{min})^{-a_{UJ}}$ and $\epsilon_\gamma = \epsilon_{\gamma,0}(\theta_j/\theta_{min})^{-b_{UJ}}$. Note that since $\epsilon = E_{iso}/4\pi \approx E/2\pi\theta_j^2$, this implies that the true energy is not necessarily constant, $E \propto \theta_j^{2-a_{UJ}}$. In order to imitate a structured jet with a uniform core, we chose

$$P(\theta_j) = \Theta(\theta_j - \theta_{min})\Theta(\theta_{max} - \theta_j)C(q)\theta_j^{-q} + B(q)\delta(\theta_j - \theta_{min}),$$
$$(6)$$

where $C(q) = [1 - B(q)](1 - q)/(\theta_{max}^{1-q} - \theta_{min}^{1-q})$ for $q \neq 1$ and $C(1) = [1 - B(1)]/\ln(\theta_{max}/\theta_{min})$ from the normalization $\int P(\theta_j)\,d\theta_j = 1$. For $P^*(L|\theta_j) = \delta[L - L(\theta_j)]$, where $L(\theta_j) = L_{min}(\theta_j/\theta_{max})^{-\lambda_{UJ}}$ and $L_{min} = L(\theta_{max})$, this implies

$$P(L) = \Theta(L - L_{min})\Theta(L_{max} - L) \frac{C\theta_{max}^{1-q}}{\lambda_{UJ}L_{min}}\left[1 - \cos\theta_j(L)\right]$$

$$\times \left(\frac{L}{L_{min}}\right)^{-1-(1-q)/\lambda_{UJ}} + B(1 - \cos\theta_{min})\delta(L - L_{max})$$

$$+ \left[B\cos\theta_{min} + C\int_{\theta_{min}}^{\theta_{max}} d\theta\theta^{-q}\cos\theta\right]\delta(L)$$

$$\approx \Theta(L - L_{min})\Theta(L_{max} - L)\frac{C\theta_{max}^{3-q}}{2\lambda_{UJ}L_{min}}\left(\frac{L}{L_{min}}\right)^{-1-(3-q)/\lambda_{UJ}}$$

$$+ B\frac{\theta_{min}^2}{2}\delta(L - L_{max})$$

$$+ \left[1 - B\frac{\theta_{min}^2}{2} - \frac{C}{2}\frac{(\theta_{max}^{3-q} - \theta_{min}^{3-q})}{(3-q)}\right]\delta(L), \quad (7)$$

---

[6] This is the standard universal structured jet model (Rossi et al. 2002; Zhang & Mészáros 2002) for $\lambda = 2$, and assuming no scatter in L for a given θ.
[7] This is a pure power law in L for all θ, instead of just for $\theta \ll 1$ as we had before.

$$P^*(L) = \Theta(L - L_{\min})\Theta(L_{\max} - L)\frac{C\theta_{\max}^{1-q}}{\lambda_{UJ}L_{\min}}\left(\frac{L}{L_{\min}}\right)^{-1-(1-q)/\lambda_{UJ}}$$
$$+ B\delta(L - L_{\max}), \tag{8}$$

where $\theta_j(L) = \theta_{\max}(L/L_{\min})^{-1/\lambda_{UJ}}$.

In the case of the structured jet discussed above, with a sharp outer edge at some finite angle $\theta_{\max}$ and a uniform core within some angle θ_c, we have

$$P(L|\theta) = \Theta(\theta_c - \theta)\delta(L - L_{\max})$$
$$+ \Theta(\theta - \theta_c)\Theta(\theta_{\max} - \theta)\delta[L - L(\theta)] + \Theta(\theta - \theta_{\max})\delta(L), \tag{9}$$

where $L(\theta) = L_{\min}(\theta/\theta_{\max})^{-\lambda_{USJ}}$ and $L_{\min} = L(\theta_{\max})$. Therefore,

$$P(L) = \Theta(L_{\max} - L)\Theta(L - L_{\min})\frac{\theta_{\max}}{\lambda_{USJ}L_{\min}}\sin\theta(L)$$
$$\times\left(\frac{L}{L_{\min}}\right)^{-1-1/\lambda_{USJ}} + (1 - \cos\theta_c)\delta(L - L_{\max})$$
$$+ \delta(L)\cos\theta_{\max}$$
$$\approx \Theta(L_{\max} - L)\Theta(L - L_{\min})\frac{\theta_{\max}^2}{\lambda_{USJ}L_{\min}}\left(\frac{L}{L_{\min}}\right)^{-1-2/\lambda_{USJ}}$$
$$+ \frac{\theta_c^2}{2}\delta(L - L_{\max}) + \left(1 - \frac{\theta_{\max}^2}{2}\right)\delta(L), \tag{10}$$

$$P^*(L) = \frac{(1 - \cos\theta_c)}{(1 - \cos\theta_{\max})}\delta(L - L_{\max})$$
$$+ \frac{\Theta(L_{\max} - L)\Theta(L - L_{\min})}{(1 - \cos\theta_{\max})\theta_{\max}^{-1}\lambda_{USJ}L_{\min}}\sin\theta(L)\left(\frac{L}{L_{\min}}\right)^{-1-1/\lambda_{USJ}}$$
$$\approx \left(\frac{\theta_c}{\theta_{\max}}\right)^2\delta(L - L_{\max}) + \Theta(L_{\max} - L)\Theta(L - L_{\min})$$
$$\times \frac{2}{\lambda_{USJ}L_{\min}}\left(\frac{L}{L_{\min}}\right)^{-1-2/\lambda_{USJ}}, \tag{11}$$

where $\theta(L) = \theta_{\max}(L/L_{\min})^{-1/\lambda_{USJ}}$ and $\int_{L_{\min}}^{\infty}P^*(L)\,dL = 1$, as it should be. Note that the coefficient in the first term in the expression for $P(L)$ includes $\theta_{\max}$ only through the combination $\theta_{\max}L_{\min}^{1/\lambda} = \theta_{\max}[L(\theta_{\max})]^{1/\lambda}$, which is independent of $\theta_{\max}$ (for a fixed normalization of L) since $L(\theta) \propto \theta^{-\lambda}$.

By comparing equations (7) and (10) one can also see that a similar luminosity function can be obtained for different values of $\lambda = a + b$, as long as $\lambda_{UJ}/\lambda_{USJ} = (3 - q)/2$. In this case, when $q \neq 1$, then $\lambda_{UJ} \neq \lambda_{USJ}$. For the same $\theta_{\max}$, $L_{\min}$, and $L_{\max}$ we have $L_{\max}/L_{\min} = (\theta_{\max}/\theta_{\min})^{\lambda_{UJ}} = (\theta_{\max}/\theta_c)^{\lambda_{USJ}}$, which implies $\theta_c/\theta_{\min} = (\theta_{\min}/\theta_{\max})^{(1-q)/2}$ (where $\theta_c < \theta_{\min}$ for $q < 1$ and $\theta_c > \theta_{\min}$ for $q > 1$). In order for the luminosity functions to be the same for the core of the structured jet, which is represented by the term $\propto \delta(L - L_{\max})$, the ratio of this term to the other terms should be the same for equations (7) and (10). Thus, we obtain

$$C(q) = \left[\frac{\theta_{\min}^{1-q}}{(3-q)} + \frac{\theta_{\max}^{1-q} - \theta_{\min}^{1-q}}{(1-q)}\right]^{-1}, \tag{12}$$

$$B(q) = \left\{1 + \frac{(3-q)}{(1-q)}\left[\left(\frac{\theta_{\max}}{\theta_{\min}}\right)^{1-q} - 1\right]\right\}^{-1}, \tag{13}$$
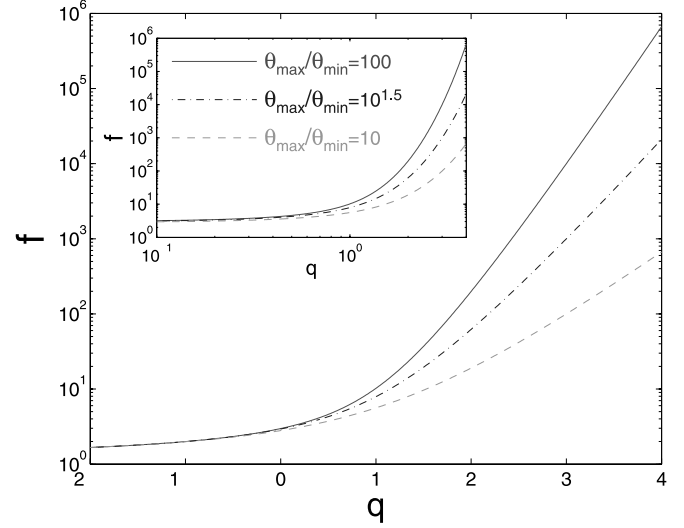

FIG. 1.—Ratio f (eq. [14]) of the true GRB rate for the UJ model to the true GRB rate for the USJ model, given the same observed GRB rate and luminosity function (i.e., the same $\log N - \log S$ distribution), as a function of the slope q of the probability distribution for the opening angle θ_j of the uniform jet, $P(\theta_j) \propto \theta_j^{-q}$ for $\theta_{\min} < \theta_j < \theta_{\max}$. See text for details. [*See the electronic edition of the Journal for a color version of this figure.*]

where $B(1) = C(1)/2 = [1 + 2\ln(\theta_{\max}/\theta_{\min})]^{-1}$ and $C(q)/B(q) = (3 - q)\theta_{\min}^{q-1}$.

The normalization of the first two terms in equation (7) for the UJ model is smaller than that of the (corresponding) first two terms in equation (10) for the USJ model by a factor of

$$f(q) = \left(\frac{\theta_{\min}}{\theta_{\max}}\right)^{1-q} + \frac{(3-q)}{(1-q)}\left[1 - \left(\frac{\theta_{\min}}{\theta_{\max}}\right)^{1-q}\right]$$
$$\approx \begin{cases} (3-q)/(1-q) & (q < 1), \\ [2/(q-1)](\theta_{\max}/\theta_{\min})^{q-1} & (q > 1), \end{cases} \tag{14}$$

where $f(1) = 1 + 2\ln(\theta_{\max}/\theta_{\min})$. This factor f is the ratio of the true GRB rate for the UJ model to the true GRB rate for the USJ model that corresponds to the same luminosity function (i.e., eqs. [7] and [10]). Figure 1 shows $f(q)$ for three different values of $\theta_{\max}/\theta_{\min}$. The fact that $f(q) > 1$ means that a larger number of uniform jets is needed, compared to structured jets, in order to reproduce the same luminosity function and the same observed rate of GRBs, $\dot{N}_{GRB}$. This means that for the same $\dot{N}_{GRB}$ the intrinsic GRB rate per unit comoving volume, $R_{GRB}(z)$, and specifically $R_{GRB}(z = 0)$, is larger by a factor f for the UJ model compared to the USJ model.

The same factor f is obtained from the ratio of the energy output in γ-rays of a single structured jet to the average energy output in γ-rays of a uniform jet. This ratio must equal the ratio of the intrinsic rates, since the total energy output in γ-rays per unit time per unit volume must be the same (Guetta et al. 2005).

We can see that $f \sim 1$ for $q < 1$ and $f \sim (\theta_{\max}/\theta_{\min})^{q-1}$ for $q > 1$. This can be understood as follows. Since most of the solid angle of the structured jet is near $\theta_{\max}$, the number of uniform jets with $\theta_j \sim \theta_{\max}$ should be comparable to the number of structured jets. Therefore, for $q < 1$, where most of the uniform jets have $\theta_j \sim \theta_{\max}$ we have $f \sim 1$, while for $q > 1$, where most of the uniform jets have $\theta_j \sim \theta_{\min}$, $f \sim (\theta_{\max}/\theta_{\min})^{q-1}$ is roughly the inverse of the fraction of jets with $\theta_j \sim \theta_{\max}$.

We have demonstrated that the luminosity function of the USJ model can be imitated by the UJ model with the appropriate choice of $P(\theta_j)$. The implied true GRB rate $R_{GRB}(z)$ for the same observed GRB rate $\dot{N}_{GRB}$ would always be larger (by a factor f) for the UJ model. For the UJ model, the term $B\delta(\theta_j - \theta_{min})$ in $P(\theta_j)$ that produces the term $\propto \delta(L - L_{max})$ in $P(L)$ is somewhat artificial and was introduced only to make a complete analogy with $P(L)$ for the USJ model. The exact form of the cutoff near θ_{min} is not clear and probably would not have a very large effect on the $\log N - \log S$ distribution, making it hard to distinguish between the two models in this way. It is also important to keep in mind that the observational constraints on the parameter a from the shape of the afterglow light curve, namely, $1.5 \lesssim a_{USJ} \lesssim 2.5$, apply only to the USJ model and not to the UJ model.

The form of the luminosity function given in equations (7) or (10) is valid only if $\theta^\lambda L(\theta) \sim const$, where $\theta = \theta_{obs}$ for the USJ model and $\theta = \theta_j$ for the UJ model. How well this condition is satisfied may be tested by using the values of both L and θ that were estimated from observations for a sample of GRBs. We consider a subsample of 19 GRBs out of the Bloom et al. (2003) sample, for which there is both a known redshift and an estimate for θ. There are larger uncertainties in the determination of the peak luminosity,[8] as the bursts were detected by different instruments with different temporal and spectral sensitivities. Following Guetta et al. (2005), we have extrapolated the GRB fluxes to the BATSE range (50–300 keV) using the method described in Sethi & Bhargavi (2001). In our analysis we have used the median value of the spectral photon index in the 50–300 keV band for the long bursts sample, -1.6, as found by Schmidt (2001). The redshifts and fluxes were taken from the table given in Van Putten & Regimbau (2003).

We calculate the values of $\theta^\lambda L$ for such a sample and for different values of λ within the range allowed for the USJ model from the constraints given above (namely, $1.5 \lesssim a_{USJ} \lesssim 2.5$ and eq. [3]): $1.83 \lesssim \lambda \lesssim 2.17$ for $k = 0$, and $1.5 \lesssim \lambda \lesssim 2.5$ for $k = 2$. Therefore, overall $1.5 < \lambda < 2.5$. The result of this analysis is that the distribution of $\theta^\lambda L(\theta)$ is not quite a delta function, and there is some dispersion around the mean value. This dispersion is reasonably fit by a lognormal distribution,

$$P(L|\theta) = \frac{1}{L\sigma\sqrt{2\pi}} \exp\left\{-\frac{[\ln L - \ln L(\theta)]^2}{2\sigma^2}\right\}, \quad (15)$$

with $L(\theta) = L_0(\theta/\theta_0)^{-\lambda}$, where $\theta_0^\lambda L_0$ is the average value of $\theta^\lambda L(\theta)$ for the observed sample and σ is the standard deviation of $\ln[\theta^\lambda L(\theta)]$, which is determined by a fit to the dispersion of the observed sample. This distribution approaches a delta function (i.e., with no scatter) for $\sigma \to 0$.

We performed fits of $\theta^\lambda L$ to a sample of 19 bursts from Bloom et al. (2003) that were observed by BATSE and *BeppoSAX*. For $\lambda = (1.5, 2, 2.5, 3)$ we obtained $\theta_0^\lambda L_0 = (15, 5.8, 2.2, 1.1) \times 10^{49}$ ergs s^{-1} and $\sigma_{obs} = (1.2, 1.2, 1.3, 1.5)$. These values of σ_{obs} can be thought of as upper limits on σ (i.e., $\sigma \lesssim \sigma_{obs}$), since the observed scatter in $\theta^\lambda L(\theta)$ includes both the intrinsic scatter (which should be reflected in σ) and additional scatter due to measurement errors in θ (which produces some scatter σ_{err}), which can be as high as tens of percent. Bloom et al. (2003) obtain a factor of 2.2 for the scatter in $\epsilon\theta^2$, implying that

$\sigma_{\ln\theta} \lesssim 0.4$, and therefore $\sigma_{err} \lesssim 0.4\lambda$.[9] Assuming that the measurement errors in θ are uncorrelated with the intrinsic scatter in $\theta^\lambda L(\theta)$, this implies $\sigma_{obs}^2 \approx \sigma^2 + \sigma_{err}^2 \lesssim \sigma^2 + (0.4\lambda)^2$, and therefore $(1.0, 0.9, 0.8, 0.9) \lesssim \sigma \lesssim (1.2, 1.2, 1.3, 1.5)$ for $\lambda = (1.5, 2, 2.5, 3)$.

The luminosity function in this case can be obtained using equations (4) and (15). It is important to note that the integral in equation (4) must be done over all possible viewing angles, even if the jet is assumed to have a core angle θ_c and maximal angle θ_{max}. In fact, together with the power-law index (λ) and normalization ($\theta_0^\lambda L_0$), the other two intrinsic parameters that define a power-law universal structured jet are the angles of its outer edge (θ_{max}) and inner core (θ_c). For the UJ model outlined above, θ_{max} and θ_c are replaced by θ_{max} and θ_{min}, which determine the range of possible θ_j values, where $P(\theta_j) \propto \theta_j^{-q}$ also depends on an additional parameter q.

The observed rate of GRBs (over the entire sky) with a peak photon flux greater than S is given by

$$\dot{N}_{GRB}(>S) = \int P(L) \, dL \int_0^{z_{max}(L,S)} \frac{R_{GRB}(z)}{(1+z)} \frac{dV(z)}{dz} \, dz, \quad (16)$$

where $P(L)$ is given by equations (4) and (15), z is the redshift of the GRB, $z_{max}(L, S)$ is the maximal redshift from which a GRB with luminosity L and peak flux S can be detected, and $R_{GRB}(z)$ is the (true) GRB rate per unit comoving volume V.[10] The factor $(1 + z)^{-1}$ accounts for the cosmological time dilation, and $dV(z)/dz$ is the comoving volume element.

4. CONSTRAINTS ON THE LUMINOSITY FUNCTION OF THE USJ MODEL

We consider all the GRBs in the GUSBAD catalog (Schmidt 2004), which lists 2204 GRBs detected at a timescale of 1024 ms. This catalog contains all the long GRBs ($T_{90} > 2$ s; Kouveliotou et al. 1993) detected while the BATSE onboard trigger (Paciesas et al. 1999) was set for 5.5 σ over background in at least two detectors, in the energy range 50–300 keV. Using this sample we estimate the ratio C_{max}/C_{min} for each burst, where C_{max} is the count rate in the second brightest illuminated detector and C_{min} is the minimum detectable rate. We find $\langle V/V_{max}\rangle = 0.335 \pm 0.007$.

We also consider the Rowan-Robinson SFR (RR-SFR; Rowan-Robinson 1999), which can be fitted with the expression

$$R_{GRB}(z) = \rho_0 \begin{cases} 10^{0.75z} & z < 1, \\ 10^{0.75} & z > 1, \end{cases} \quad (17)$$

where $\rho_0 = R_{GRB}(z = 0)$ is the true GRB rate per unit comoving volume at $z = 0$. Throughout the paper we use the following cosmological parameters: $(\Omega_M, \Omega_\Lambda, h) = (0.3, 0.7, 0.7)$.

Objects with luminosity L observed by BATSE with a flux limit S_{lim} are detectable to a maximum redshift $z_{max}(L, S_{lim})$. The limiting flux has a distribution $G(S_{lim})$ that can be obtained from the distribution of C_{min} of the GUSBAD catalog. Considering five main representative intervals we obtain that 30%, 30%, 10%, 20%, and 10% of the sample have $S_{lim} \sim 0.23, 0.25,$

---

[8] We use the peak luminosity since it is usually the most relevant quantity for the triggering of the different detectors.

[9] This is because the dominant measurement error in $\theta^\lambda L$ comes from θ^λ, while L is measured more accurately.

[10] Note that $R_{GRB}(z)$ is the true GRB rate, and it is obtained directly from this formalism without any need for a "correction factor," etc.

0.22, 0.26, and 0.27 photons cm^{-2} s^{-1}, respectively. Therefore, we have

$$\dot{N}_{\mathrm{GRB}}(>S) =$$

$$\int P(L)\,dL \int G(S_{\mathrm{lim}})\,dS_{\mathrm{lim}} \int_0^{z_{\max}[L,\,\max(S,\,S_{\mathrm{lim}})]} \frac{R_{\mathrm{GRB}}(z)}{(1+z)}\,\frac{dV(z)}{dz}\,dz$$

$$= \int P(L)\,dL \left[\int_0^S G(S_{\mathrm{lim}})\,dS_{\mathrm{lim}} \int_0^{z_{\max}(L,\,S)} \frac{R_{\mathrm{GRB}}(z)}{(1+z)}\,\frac{dV(z)}{dz}\,dz \right.$$

$$\left. + \int_S^{\infty} G(S_{\mathrm{lim}})\,dS_{\mathrm{lim}} \int_0^{z_{\max}(L,\,S_{\mathrm{lim}})} \frac{R_{\mathrm{GRB}}(z)}{(1+z)}\,\frac{dV(z)}{dz}\,dz \right],$$

$$(18)$$

where $P(L)$ is given by equation (4). For the USJ model $P(L|\theta > \theta_{\max}) = \delta(L)$, while $P(L|\theta < \theta_{\max})$ is given by equation (15) with $L(\theta) = L_{\max} \min[1, (\theta/\theta_{\min})^{-\lambda_{\mathrm{USJ}}}]$, where $L_{\max} = L_{\min}(\theta_{\min}/\theta_{\max})^{-\lambda_{\mathrm{USJ}}}$. A similar dispersion is introduced in the UJ model. The predicted $\log N - \log S$ distribution depends on the values of λ_{USJ}, θ_c, $\theta_{\max}$, σ, and the normalization $\theta_0^{\lambda_{\mathrm{USJ}}} L_0$, where the last parameter is determined through a fit to observations and is not considered to be a free parameter. The scatter σ is constrained by observations, $(1.0, 0.9, 0.8, 0.9) \lesssim \sigma \lesssim (1.2, 1.2, 1.3, 1.5)$ for $\lambda_{\mathrm{USJ}} = (1.5, 2, 2.5, 3)$, but was allowed to vary over a wider range when performing the fit to the data. The smallest observed values of θ provide an upper limit on θ_c of $\theta_c \lesssim 0.05$, while the largest observed values of θ provide a lower limit on $\theta_{\max}$ of $\theta_{\max} \gtrsim 0.5$. For the USJ model the shape of the afterglow light curves implies $1.5 \lesssim a_{\mathrm{USJ}} \lesssim 2.5$, and therefore $1.5 \lesssim \lambda_{\mathrm{USJ}} \lesssim 2.5$; however, since this limit does not apply to the UJ model, and since we wanted to properly check the consistency of the USJ with the data, we allowed λ_{USJ} to vary over a wider range when performing the fit to the data.

Combining the constraint from the Frail et al. (2001) relation (eq. [3]) with the limit on λ from the luminosity function allows us to separately constrain a and b. From equation (3) we have $a = 2(4-k) - (3-k)\lambda = 8 - 3\lambda$ for $k = 0$ and $4 - \lambda$ for $k = 2$. Since for the USJ model $1.5 \lesssim a_{\mathrm{USJ}} \lesssim 2.5$ from the afterglow light curves, this implies $11/6 \lesssim \lambda_{\mathrm{USJ}} \lesssim 13/6$ for $k = 0$ and $1.5 \lesssim \lambda_{\mathrm{USJ}} \lesssim 2.5$ for $k = 2$. For $k = 0$, λ must be close to 2 and $b = (4-k)(\lambda - 2)$ falls in the range $-2/3 \lesssim b \lesssim 2/3$. For $k = 2$ this implies $-1 \lesssim b \lesssim 1$. As discussed in § 2, direct estimates of ϵ_γ suggest $0 \lesssim b \lesssim 1$ (this applies both to the USJ model and to the UJ model). The different constraints on the parameters a and b are summarized in Figure 5.

If the luminosity function forces λ_{USJ} to values less than 2, then b must be negative, and if λ_{USJ} approaches 1.5, this would favor an external medium with a $k = 2$ density profile. Note that $b < 0$ corresponds to the dissipation efficiency increasing with angle, as would be expected if it is associated with a shear layer well outside the jet core. We note that highly relativistic jets passing through an external pressure gradient less steep than r^{-4} can develop a shocked layer near the jet boundary because of the loss of causal contact between the jet interior and wall. If this shock is responsible for the γ-ray emission, it could lead to radiative efficiency increasing with θ.

On the other hand, if the luminosity function implies $\lambda_{\mathrm{USJ}} > 2$, this would imply $b > 0$, i.e., a γ-ray efficiency ϵ_γ that decreases with θ, which is more consistent with direct estimates of ϵ_γ. If λ_{USJ} approaches 2.5, this would favor a $k = 2$ density profile.

We performed two fits to the data using a single power-law luminosity function that can arise either in the USJ model or in the UJ model. In the first fit we let all four free parameters vary: λ_{USJ}, θ_c, $\theta_{\max}$, and σ. In the second fit we held the value of λ fixed at $\lambda_{\mathrm{USJ}} = 2$ and allowed the remaining three parameters to vary: θ_c, $\theta_{\max}$, and σ. The second fit was performed since a value of $\lambda_{\mathrm{USJ}} = 2$ is expected in the simplest version of the USJ model, where the γ-ray efficiency ϵ_γ is constant ($b_{\mathrm{USJ}} = 0$), and therefore $a_{\mathrm{USJ}} = \lambda_{\mathrm{USJ}} = 2$ because of the Frail et al. (2001) relation (eq. [3]). Therefore, it is interesting to test whether this simplest version of the USJ model is consistent with the observed $\log N - \log S$ distribution.

In order to assign a χ^2 value to the fit we divided the 2204 GRBs in the GUSBAD catalog into 14 bins according to their value of S, the peak photon flux. The first 11 bins are equally spaced in $\log S$. In the remaining 3 bins, which correspond to the highest values of S, we chose a larger range of S values so as to have at least $N_{\min} = 40$ GRBs in each bin, in order to have reasonable Poisson statistics. Since the overall normalization is an additional free parameter in our fits, the number of degrees of freedom (dof) in our fits is $\nu = 14 - (4 + 1) = 9$ in our first fit, and $\nu = 10$ in our second fit.

The results of the fits are presented in Table 1 and in Figures 2 and 3. When λ is free to vary we obtain a best-fit value of $\lambda_{\mathrm{USJ}} = 2.9^{+0.2}_{-0.5}$; however, when we fix $\lambda_{\mathrm{USJ}} = 2$ we still get an acceptable fit. This suggests that although values of $\lambda_{\mathrm{USJ}} > 2$ are preferred by the data, a value of $\lambda_{\mathrm{USJ}} = 2$ is still possible. On the other hand, values of $\lambda_{\mathrm{USJ}} < 2$ become increasingly harder to reconcile with the data. Values of $\lambda_{\mathrm{USJ}} > 2$, which are preferred by the data, correspond to $b > 0$ (a γ-ray efficiency ϵ_γ that decreases with θ) and for the USJ model $\lambda_{\mathrm{USJ}} \approx 2.5$ favors $k = 2$ (i.e., a stellar wind external density profile).

The first fit gives $\sigma = 0.5^{+0.7}_{-0.5}$, which indicates that this fit is not very sensitive to the value of σ. It also includes the range $0.8 \lesssim \sigma \lesssim 1.3$ for $\lambda_{\mathrm{USJ}} = 2.5$ and $0.9 \lesssim \sigma \lesssim 1.5$ for $\lambda_{\mathrm{USJ}} = 2.9$ that are implied by observations. In contrast, the second fit with a fixed $\lambda_{\mathrm{USJ}} = 2$ gives $\sigma = 0.8^{+0.4}_{-0.2}$, which requires a positive value of σ in order to get a reasonable fit to the data.

The best-fit values of θ_c and $\theta_{\max}$ are slightly higher for the first fit, but are rather close between the two fits. The best-fit values of $\theta_c = 0.05^{+0.005}_{-0.01}$ for a free λ and $\theta_c = 0.03^{+0.005}_{-0.01}$ for a fixed $\lambda_{\mathrm{USJ}} = 2$ are close to the upper limit of $\theta_c \lesssim 0.05$ from observations, and the allowed confidence regions do not allow values much smaller (by more than a factor of ~2) than this limit. The best-fit values of $\theta_{\max} = 0.7 \pm 0.2$ for a free λ and $\theta_{\max} = 0.5 \pm 0.05$ for a fixed $\lambda_{\mathrm{USJ}} = 2$ are close to the lower limit of $\theta_{\max} \gtrsim 0.5$ from observations and are not consistent with $\theta_{\max} = \pi/2$.

The true GRB rate that is implied from our fits is rather close to the value of $R_{\mathrm{GRB}}(z = 0) \sim 0.5$ Gpc^{-3} yr^{-1} that was found by Perna et al. (2003). We obtain a slightly larger rate for the free λ fit compared to the fixed $\lambda_{\mathrm{USJ}} = 2$ fit, but the difference is very small. The rates we obtain for the USJ model are lower by a factor of ~300 compared to the estimate of Frail et al. (2001) for the UJ model.

Finally, since the exact choice for the number and sizes of the bins used in our fit is somewhat arbitrary and might have some effect on our results, we estimate this effect more quantitatively by repeating our fit for a single power-law luminosity function with a larger number of bins, 26 instead of 14 (see Fig. 4). The best-fit parameter values remained the same as for the original binning (14 bins) up to the significant digits shown in Table 1, while the 1 σ confidence intervals slightly changed: $\lambda_{\mathrm{USJ}} = 2.9^{+0.2}_{-0.4}$, $\sigma = 0.5^{+0.7}_{-0.4}$, $\theta_c = 0.05 \pm 0.05$, and $\theta_{\max} = 0.7^{+0.2}_{-0.1}$. The

TABLE 1
Fits to the $\log N - \log S$ Distribution

$P(L)$ Model	Model Parameters	$R_{\mathrm{GRB}}(z = 0)$ (Gpc^{-3} yr^{-1})	Goodness of Fit
Single power law	$\lambda_{\mathrm{USJ}} = 2.9^{+0.2}_{-0.5}$	$0.86^{+0.14}_{-0.05}$ (USJ)	$\chi^2 = 11.05$ (9 dof)
	$\sigma = 0.5^{+0.7}_{-0.5}$	$5.4^{+1.8}_{-1.0}$ (UJ, $q = 1$)	$P = 0.723$ (1.10 σ)
	$\theta_c = 0.05^{+0.005}_{-0.01}$	...	...
	$\theta_{\max} = 0.7 \pm 0.2$	...	...
Single power law + fixed λ_{USJ}	$\lambda_{\mathrm{USJ}} = 2$ (fixed)	$0.75^{+0.07}_{-0.06}$ (USJ)	$\chi^2 = 14.67$ (10 dof)
	$\sigma = 0.8^{+0.4}_{-0.2}$	$5.0^{+1.3}_{-0.8}$ (UJ, $q = 1$)	$P = 0.855$ (1.46 σ)
	$\theta_c = 0.03^{+0.005}_{-0.01}$	...	...
	$\theta_{\max} = 0.5 \pm 0.05$	...	...
Double power law + $\sigma = 0$	$\alpha = 0.6 \pm 0.1$	10.7 ± 2.3 (UJ, $q = 1$)	$\chi^2 = 10.57$ (10 dof)
	$\beta = 0.8^{+0.2}_{-0.1}$	...	$P = 0.608$ (0.86 σ)
	$L_{51} = 1.6^{+0.8a}_{-0.6}$	...	...
	...	...	...

Notes.—The best-fit parameters with their 1 σ confidence intervals are shown together with the implied true GRB rate and the goodness of fit. The confidence intervals are the projection onto the relevant parameter axis of the region in the multidimensional parameter space around the global minimum $\chi^2_{\min}$ of χ^2, where $\Delta\chi^2 = \chi^2 - \chi^2_{\min} < 1$.

[a] Here $L_{51} = L_*/(10^{51}$ ergs s$^{-1})$.

GRB rate is slightly higher, $R_{\mathrm{GRB}}(z = 0) = 0.95^{+0.25}_{-0.22}$ Gpc^{-3} yr^{-1}, but well within the 1 σ confidence interval for the original binning. This demonstrates that while the exact choice of binning has some effect on our results, this effect is rather small.

In order to estimate the effect of our choice for the star formation rate (or more accurately the GRB rate that is assumed to follow the star formation rate up to an unknown normalization constant) we repeated our fit with the original binning (14 bins) but with a different star formation rate: SFR2 from Porciani & Madau (2001). We obtained $\lambda_{\mathrm{USJ}} = 2.9^{+0.3}_{-0.4}$, $\sigma = 0.5 \pm 0.5$, $\theta_c = 0.04 \pm 0.005$, and $\theta_{\max} = 0.9 \pm 0.2$. While changing the star formation rate has a larger effect than changing the binning, the parameter values for the two different star formation rates that we considered are still consistent with each other within their 1 σ confidence intervals. For the new star formation

rate we obtain a slightly lower true GRB rate, $R_{\mathrm{GRB}}(z = 0) = 0.65^{+0.05}_{-0.17}$ Gpc^{-3} yr^{-1}.

5. THE LUMINOSITY FUNCTION FOR THE UNIFORM JET MODEL

The two fits that were discussed in § 4 for the USJ model still apply to the UJ model with $\theta_c \to \theta_{\min}$ and $\lambda_{\mathrm{USJ}} \to \lambda_{\mathrm{UJ}} \times 2/(3 - q)$. The second substitution indicates a degeneracy where the luminosity function $P(L)$ and therefore the $\log N - \log S$ distribution would be the same for UJ models with the same value of $\lambda_{\mathrm{UJ}}/(3 - q) = (a_{\mathrm{UJ}} + b_{\mathrm{UJ}})/(3 - q)$. This degeneracy does not enable us to determine $P(\theta_j)$, which is parameterized by q from a fit to the observed $\log N - \log S$ distribution. Such a fit can only determine $\eta = 1 + 2/\lambda_{\mathrm{USJ}} = 1 + (3 - q)/\lambda_{\mathrm{UJ}}$, where $P(L) \propto L^{-\eta}$. The degeneracy might be broken if we could estimate the

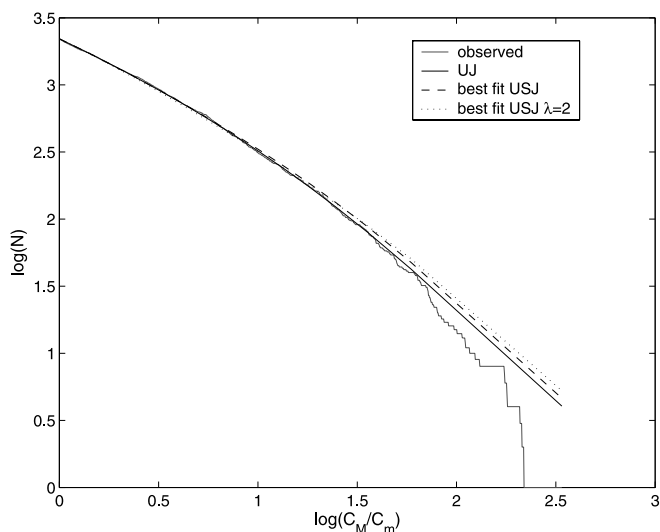Fig. 2.—Observed cumulative $\log_{10}N - \log_{10}(C_{\max}/C_{\min})$ distribution taken from the GUSBAD catalog (*solid steplike line*) compared to the predicted $\log_{10}N - \log_{10}(P/P_{\lim})$ distributions for our best-fit models: a single power-law luminosity function (relevant for both the USJ and the UJ models), both when letting all parameters vary (*dashed line*) and when fixing $\lambda_{\mathrm{USJ}} = 2$ (*dotted line*), and a broken power-law luminosity function (*solid line*; relevant only for the UJ model). [*See the electronic edition of the Journal for a color version of this figure.*]
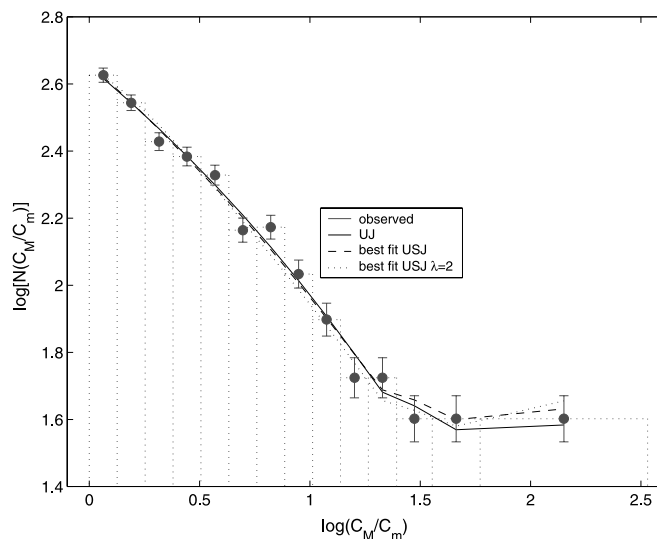

Fig. 3.—Same as Fig. 2, but for the differential distribution: $\log_{10}(P/P_{\lim})$ is divided into 14 bins, the first 11 of equal size, and the remaining 3 with varying sizes chosen such that the number of bursts per bin in the observed sample is at least $N_{\min} = 40$ (in order to have reasonable statistics so that the Poisson error will not to be too large), and N is the observed (*circles*) or theoretical (*lines*; only the values at the center of each bin count) number of bursts in each bin. The edges of the bins are also plotted. [*See the electronic edition of the Journal for a color version of this figure.*]
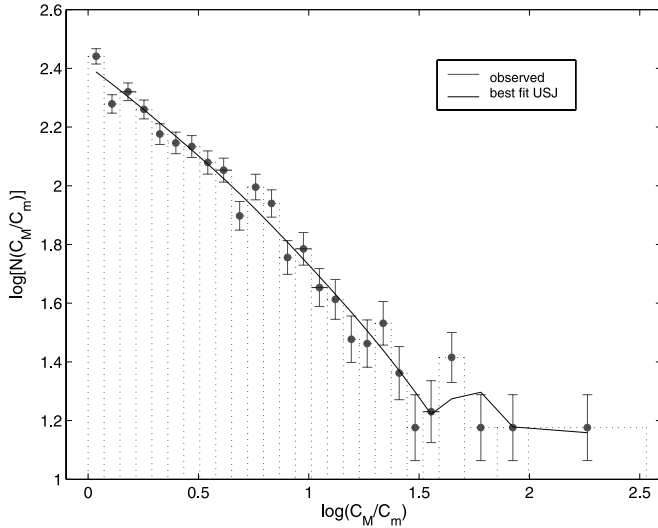
FIG. 4.—Same as Fig. 3, but for a different binning of $\log_{10}(P/P_{\lim})$: 26 bins and $N_{\min} = 15$. [*See the electronic edition of the Journal for a color version of this figure.*]

true GRB rate in an independent way. This is since the true GRB rate for the USJ model is determined from the fit to the observed $\log N - \log S$ distribution, and the correction factor for the UJ model depends only on q (see eq. [14] and Fig. 1). Thus, an independent estimate of the true GRB rate would enable the determination of q and would therefore constrain $P(\theta_j)$.

The value of $\lambda = a + b$ is the same for the UJ and USJ models if and only if $q = 1$. In fact, the Frail et al. (2001) relation as manifested in equation (3) implies that for $q = 1$ and a given value of k, it is enough that either a or b be the same for the two models in order for $\lambda = a + b$ to be the same. Add to this the fact that for $q = 1$ there is an equal number of uniform jets per logarithmic interval in θ_j, and $q = 1$ might be considered as the most "natural" value for q. However, we emphasize that there is no physical basis for comparing pairs of models with $\lambda_{USJ} = \lambda_{UJ}$, and therefore no a priori reason for choosing $q = 1$. The only meaningful comparison is to observations.

The discussion in § 4 about the values of λ_{USJ}, σ, $\theta_{\max}$, and θ_c for the USJ model are still valid for the UJ model, where θ_c is replaced by $\theta_{\min}$ and λ_{USJ} is replaced by $2\lambda_{UJ}/(3 - q)$. The true GRB rate for the UJ model is higher than that for the USJ model for the same fit to the observed $\log N - \log S$ distribution by a factor $f(q)$, which is given in equation (14) and shown in Figure 1. In Table 1 we provide the values for $q = 1$ as an example. The true GRB rate that we obtain for $q = 1$ is a factor of ≈ 6–6.6 lower than that of Guetta et al. (2005) and a factor of ≈ 45–50 smaller than that of Frail et al. (2001). However, since the GRB rate that is obtained in this way has a strong dependence on the value of q (see Fig. 1), the rates for $q = 1$ are not very meaningful (as discussed in the previous paragraph). A constant efficiency ($b = 0$) and a constant energy ($a = 2$) imply $\lambda_{UJ} = 2$, which, together with the best-fit value of $\lambda_{USJ} \approx 2.9$, give $q = 3 - 2\lambda_{UJ}/\lambda_{USJ} \approx 1.6$. For the best-fit parameter values this would imply $f(q) \approx 14.4$ and a true GRB rate of $R_{GRB}(z = 0) \approx 12.3$ Gpc^{-3} yr^{-1}.

It is remarkable that we obtain a good fit to the data for the UJ model for a single power-law distribution of jet half-opening angles, $P(\theta_j)$, and a scatter σ in the peak luminosity for a given θ_j that is consistent with observations. Previous works used a

broken power-law luminosity function $P(L)$, which corresponds to a broken power law $P(\theta_j)$, and no scatter ($\sigma = 0$). For this reason, we also performed a fit with $\sigma = 0$ and a broken power-law luminosity function $P(L)$ with the parameterization of Guetta et al. (2005), where[11] $P(L) \propto L^{-1-\alpha}$ for $L < L_*$, and $P(L) \propto L^{-1-\beta}$ for $L > L_*$. The results of this fit are shown in Table 1 and Figures 2 and 3. We get a good fit where $\alpha = 0.6 \pm 0.1$ and $\beta = 0.8^{+0.2}_{-0.1}$ are consistent with having the same value, $\alpha \approx \beta \approx 0.7$. This last value implies $\eta \approx 1.7$, which is consistent with our best-fit value of $\lambda_{USJ} = 2.9$, which implies $\eta = 1 + 2/\lambda_{USJ} \approx 1.7$. This suggests that a broken power law is not really necessary, and a single power law can provide a reasonable fit to the data even for $\sigma = 0$ (as we obtain for the first $\lambda_{USJ} = 2$ fit from the previous section, with different $L_{\min}$ and $L_{\max}$, which correspond to different $\theta_{\max}$ and θ_c).

6. DISCUSSION

We have developed a formalism that enables us to calculate the theoretical $\log N - \log S$ distribution for any GRB jet structure and directly provides the true GRB rate from a fit to the observed $\log N - \log S$ distribution. This is a more straightforward approach compared to previous works (Schmidt 2001; Guetta et al. 2005), which first calculated the GRB rate assuming an isotropic emission and then introduced a "correction factor" in order to account for the effects of the GRB jet structure. We have applied this formalism to the uniform jet (UJ) model and to the universal structured jet (USJ) model and performed fits to the GUSBAD catalog, which includes 2204 BATSE bursts. Our analysis improves on previous works by (1) allowing the efficiency in producing γ-rays to vary with θ, (2) including an internal dispersion in the peak luminosity L at any given θ, (3) introducing an inner core angle θ_c and an outer edge $\theta_{\max}$ in the USJ model, and (4) using a larger and more uniform GRB sample. The results of our fits are summarized in Table 1 and Figures 2 and 3.

A power-law luminosity function has also been fitted to the $\log N - \log S$ distribution in some previous works (Hakkila et al. 1996; Loredo & Wasserman 1998; Stern et al. 2002, hereafter STS02). Of these works, it is most useful to compare our results to those of STS02, since their assumptions are the closest to ours: like us, they assumed $(\Omega_M, \Omega_\Lambda) = (0.3, 0.7)$ and that the GRB rate follows the star formation rate. It is important to keep in mind, however, that STS02 used a different GRB sample. STS02 obtained a power-law luminosity function at low luminosities, with an index of $\eta = 1.4$, where $P(L) \propto L^{-\eta}$. This is rather close to the power-law index of $\eta = 1.7$ (or between 1.6 and 1.8 at 1 σ) that we obtain over the whole luminosity range for a single power-law luminosity function. It is also close to the power-law index of $\eta = 1.6$ (or between 1.5 and 1.7 at 1 σ) that we obtain for low luminosities when using a broken power-law luminosity function. Also, for a single power law, we have a maximal luminosity (corresponding to the core angle θ_c in the USJ model or the minimal jet half-opening angle $\theta_{\min}$ in the UJ model) with and exponential tail [due to the assumed scatter around the mean value of $L(\theta)$], which is not very different from an exponential cutoff (or decline) at high luminosities, that was found to be a viable option by STS02. Thus, we conclude that our results are consistent with those of STS02.

---

[11] Here we define α and β with a minus sign with respect to their definition in Guetta et al. (2005).

The main differences between our work and previous works in the literature that aimed constraining the GRB luminosity function using the peak flux distribution are (1) the different sample that we use and (2) the fact that we consider a differential peak flux distribution instead of the cumulative distribution, since random errors propagate in an unknown way in the cumulative distribution. Moreover, unlike previous authors, we consider the possibility that the jet is structured and derive the corresponding luminosity function, which in turn puts constraints on the jet structure through the fit to the $\log N - \log S$ distribution.

The values we obtain for θ_c in the USJ model or $\theta_{\min}$ in the UJ model are close to the upper limit of ~ 0.05 that is implied by the smallest values of θ that are inferred from afterglow observations. Furthermore, they are not consistent with zero. The value of $\theta_{\max}$ that we obtain is close to the lower limit of ~ 0.5 from afterglow observations and is not consistent with $\pi/2$. Therefore, we find that including θ_c (or $\theta_{\min}$) and $\theta_{\max}$ is required in order to obtain a good fit to the data.

We fit the observed distribution of $\theta^\lambda L(\theta)$ (where L is the peak luminosity) for a sample of 19 GRBs with a known redshift z and an estimate for θ, to a lognormal distribution with a standard deviation σ. We found the fit to a lognormal distribution to be acceptable. The implied values of σ are $(1.0, 0.9, 0.8, 0.9) \lesssim \sigma \lesssim (1.2, 1.2, 1.3, 1.5)$ for $\lambda = (1.5, 2, 2.5, 3)$, where we have taken into account that part of the observed dispersion might arise because of error in the estimated value of θ. This is consistent with the wide range of possible σ values we obtain in our fit for a free λ, $\sigma = 0.5^{+0.7}_{-0.5}$, and with the smaller range of values for our fit with a fixed $\lambda_{\mathrm{USJ}} = 2$, $\sigma = 0.8^{+0.4}_{-0.2}$.

The Frail et al. (2001) relation constrains the values of the power-law indices a and b of the energy per solid angle in the jet (ϵ) and the γ-ray efficiency (ϵ_γ), respectively (see eq. [3]). For the USJ model the observed shapes of the afterglow light curves imply $1.5 \lesssim a_{\mathrm{USJ}} \lesssim 2.5$ (Granot & Kumar 2003; Kumar & Granot 2003), which in turn implies $11/6 \lesssim \lambda_{\mathrm{USJ}} \lesssim 13/6$ and $-2/3 \lesssim b_{\mathrm{USJ}} \lesssim 2/3$ for $k = 0$ or $1.5 \lesssim \lambda_{\mathrm{USJ}} \lesssim 2.5$ and $-1 \lesssim b_{\mathrm{USJ}} \lesssim 1$ for $k = 2$. As discussed in § 2, direct estimates of ϵ_γ from afterglow observations suggest $0 \lesssim b \lesssim 1$. Our best-fit value of $\lambda_{\mathrm{USJ}} = 2.9^{+0.2}_{-0.5}$ favors a stellar wind external density profile ($k = 2$) and an efficiency that decreases with θ ($b > 0$). However, $\lambda_{\mathrm{USJ}} = 2$, which corresponds to $b = 0$ and does not constrain the value of k, still provides an acceptable fit to the data. The constraints on a and b are summarized in Figure 5.

For the UJ model we find a degeneracy in the luminosity function, $P(L) \propto L^{-\eta}$, where $\eta = 1 + (3 - q)/\lambda_{\mathrm{UJ}}$ and $\lambda_{\mathrm{UJ}} = a_{\mathrm{UJ}} + b_{\mathrm{UJ}}$. Since a fit to the observed $\log N - \log S$ distribution can only constrain the luminosity function $P(L)$, in our case it can only provide the value of η. However, this constrains only the value of $(3 - q)/\lambda_{\mathrm{UJ}} = (3 - q)/(a_{\mathrm{UJ}} + b_{\mathrm{UJ}})$, and therefore still does not enable us to determine the values q and λ_{UJ} separately. An independent estimate of the true GRB rate would constrain $f(q)$ and therefore q, and would thus enable one to break this degeneracy.

Alternatively, one can make an additional assumption on a_{UJ} or b_{UJ}. The true energy in the jet scales as $E \propto \theta_j^{2-a_{\mathrm{UJ}}}$ and a constant energy corresponds to $a_{\mathrm{UJ}} = 2$. If we assume a constant energy, the Frail et al. (2001) relation (eq. [3]) implies a constant efficiency ($b_{\mathrm{UJ}} = 0$), and vice versa. In this case $\lambda_{\mathrm{UJ}} = 2$ and the best-fit value of $\eta = 1 + 2/\lambda_{\mathrm{USJ}} \approx 1.7$ implies $q \approx 1.6$. For the best-fit parameter values this would imply
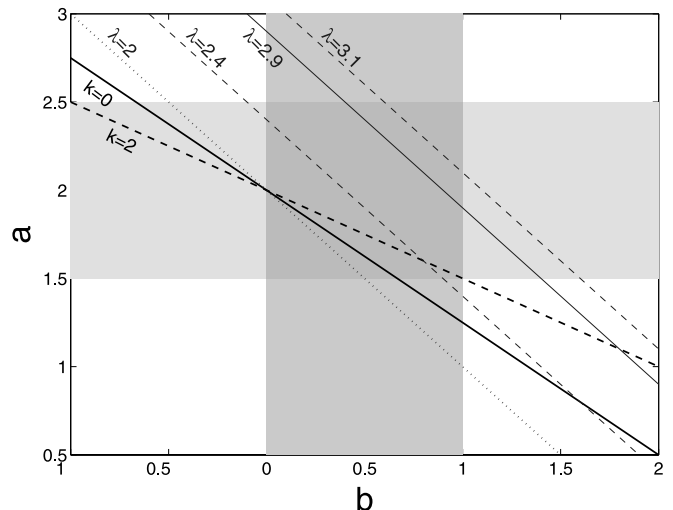

Fig. 5.—Summary of the constraints on the power-law indices a and b of the kinetic energy per solid angle and the γ-ray efficiency, respectively: $\epsilon \propto \theta^{-a}$ and $\epsilon_\gamma \propto \theta^{-b}$, where $\theta = \theta_{\mathrm{obs}}$ for the USJ model and $\theta = \theta_j$ for the UJ model. The constraint from the Frail et al. (2001) relation (eq. [3]) is shown both for a constant density external medium ($k = 0$) and for a stellar wind environment ($k = 2$). Also shown are the values of $\lambda = a + b$ for the best-fit value ($\lambda_{\mathrm{USJ}} = 2.9$) and the $1\,\sigma$ confidence interval ($2.4 < \lambda_{\mathrm{USJ}} < 3.1$) for the USJ model, as well as $\lambda = 2$, which is still acceptable. The shaded regions show the constraints $1.5 \lesssim a_{\mathrm{USJ}} \lesssim 2.5$ from the afterglow light curves, which applies only to the USJ model, and $0 \lesssim b \lesssim 1$ from estimates of the γ-ray efficiency, which applies to both the USJ model and the UJ model. The intersection of these two shaded regions is indicated. [*See the electronic edition of the Journal for a color version of this figure.*]

$f(q) \approx 14.4$ and a true GRB rate of $R_{\mathrm{GRB}}(z = 0) \approx 12.3$ Gpc^{-3} yr^{-1}. This last value is a factor of ≈ 2.7 lower than that of Guetta et al. (2005) and a factor of ≈ 20 smaller than that of Frail et al. (2001). It is also a factor of $\approx 4.9 \times 10^3$ smaller than the rate of SNe Type Ib/c, $R_{\mathrm{SN\,Ib/c}}(z = 0) \approx 6 \times 10^4$ Gpc^{-3} yr^{-1}.

For $a_{\mathrm{UJ}} = 2$ and $b_{\mathrm{UJ}} = 0$, the $1\,\sigma$ confidence interval of $2.4 < \lambda_{\mathrm{USJ}} < 3.1$ in λ_{USJ} corresponds to $1.3 < q < 1.7$, $9.5 < f(q) < 16.5$, and $R_{\mathrm{GRB}}(z = 0) \cong (7.7–16.5)$ Gpc^{-3} yr^{-1}. These values of q are not very far from $q = 1$ for which there is an equal number of jets per logarithmic interval in θ_j. It implies that there are more jets with $\theta_j \sim \theta_{\min}$ compared to $\theta_j \sim \theta_{\max}$, by a factor of $\sim (\theta_{\max}/\theta_{\min})^{q-1} \sim (2.1–9.1)$, where $9 \lesssim \theta_{\max}/\theta_{\min} \lesssim 23$ (see Table 1). If we allow the value of either a_{UJ} or b_{UJ} to vary, they must both vary together in order to satisfy the Frail et al. (2001) relation (eq. [3]). This would cause the values of q, $f(q)$, and the true GRB rate for the UJ model to all vary accordingly. The strong dependence of $f(q)$ on q (see Fig. 1) implies that this can potentially increase the true GRB rate by a large factor. The fact that $f(q) > 1$ for all q implies that the true GRB rate for the USJ model, which is given in Table 1, provides a lower limit for the UJ model.

REFERENCES

Bloom, J. S., Frail, D. A., & Kulkarni, S. R. 2003, ApJ, 594, 674
Firmani, C., Avila-Reese, V., Ghisellini, G., & Tutukov, A. V. 2004, ApJ, 611, 1033
Frail, D. A., et al. 2001, ApJ, 562, L55
Granot, J., & Königl, A. 2003, ApJ, 594, L83
Granot, J., & Kumar, P. 2003, ApJ, 591, 1086
Granot, J., Miller, M., Piran, T., Suen, W. M., & Hughes, P. A. 2001, in Gamma-Ray Bursts in the Afterglow Era, ed. E. Costa, F. Frontera, & J. Hjorth (Berlin: Springer), 312
Granot, J., Panaitescu, A., Kumar, P., & Woosley, S. E. 2002, ApJ, 570, L61
Guetta, D., Piran, T., & Waxman, E. 2005, ApJ, in press
Guetta, D., Spada, M., & Waxman, E. 2001, ApJ, 557, 399
Hakkila, J., et al. 1996, ApJ, 462, 125
Kouveliotou, C., et al. 1993, ApJ, 413, L101
Kumar, P., & Granot, J. 2003, ApJ, 591, 1075
Kumar, P., & Panaitescu, A. 2000, ApJ, 541, L9
Lipunov, V. M., Postnov, K. A., & Prokhorov, M. E. 2001, Astron. Rep., 45, 236
Lloyd-Ronning, N. M., & Zhang, B. 2004, ApJ, 613, 477
Loredo, T. J., & Wasserman, I. M. 1998, ApJ, 502, 75
Moderski, R., Sikora, M., & Bulik, T. 2000, ApJ, 529, 151

Nakar, E., Granot, J., & Guetta, D. 2004, ApJ, 606, L37
Paciesas, W., et al. 1999, ApJS, 122, 465
Panaitescu, A., & Kumar, P. 2001, ApJ, 554, 667
———. 2002, ApJ, 571, 779
Panaitescu, A., & Mesźaros, P. 1999, ApJ, 526, 707
Perna, R., Sari, R., & Frail, D. 2003, ApJ, 594, 379
Porciani, C., & Madau, P. 2001, ApJ, 548, 522
Rhoads, J. E. 1997, ApJ, 487, L1
———. 1999, ApJ, 525, 737
Rossi, E., Lazzati, D., & Rees, M. J. 2002, MNRAS, 332, 945
Rossi, E., Lazzati, D., Salmonson, J. D., & Ghisellini, G. 2004, MNRAS, 354, 86
Rowan-Robinson, M. 1999, Ap&SS, 266, 291
Sari, R. 1997, ApJ, 489, L37
Sari, R., Piran, T., & Halpern, J. 1999, ApJ, 519, L17
Schmidt, M. 2001, ApJ, 552, 36
———. 2004, ApJ, submitted (astro-ph/0406519)
Sethi, S., & Bhargavi, S. G. 2001, A&A, 376, 10
Stern, B. E., Tikhomirova, Ya., & Svensson, R. 2002, ApJ, 573, 75 (STS02)
Van Putten, M., & Regimbau, T. 2003, ApJ, 593, L15
Zhang, B., & Mészáros, P. 2002, ApJ, 571, 876